ACS APPLIED MATERIALS & INTERFACES

Research Article

www.acsami.org

Delivery of Paclitaxel Using PEGylated Graphene Oxide as a Nanocarrier

Zhiyuan Xu,[†,‡] Shaojia Zhu,[‡] Mingwei Wang,[§] Yongjun Li,[†] Ping Shi,*[,‡] and Xiaoyu Huang*[,†]

[†]Key Laboratory of Synthetic and Self-Assembly Chemistry for Organic Functional Molecules, Shanghai Institute of Organic Chemistry, Chinese Academy of Sciences, 345 Lingling Road, Shanghai 200032, People's Republic of China

[‡]State Key Laboratory of Bioreactor Engineering, East China University of Science and Technology, 130 Meilong Road, Shanghai 200237, People's Republic of China

[§]Department of Nuclear Medicine, Fudan University Shanghai Cancer Center, 270 Dongan Road, Shanghai 200032, People's Republic of China

ABSTRACT: Paclitaxel (PTX) is an extensively used potent chemotherapy drug; however, low water solubility, poor bioavailability, and emergence of drug resistance in patients limited its biological application. In this report, we proposed a new drug delivery system for cancer therapy based on graphene oxide (GO), a novel 2D nanomaterial obtained from the oxidation of natural graphite, to improve the utilization rate of PTX. PTX was first connected to biocompatible 6-armed poly(ethylene glycol), followed by covalent introduction into the surface of GO sheets via a facile amidation process under mild conditions, affording the drug delivery system, GO-PEG-PTX (size 50−200 nm). GO-PEG nanosized carrier could quickly enter into human lung cancer A549 and human breast cancer MCF-7 cells verified by inverted fluorescence microscope using fluorescein isothiocyanate as probe. This nanocarrier was nontoxic to A549 and MCF-7 cells without linking with PTX. Nevertheless, GO-PEG-PTX showed remarkably high cytotoxicity to A549 and MCF-7 cells in a broad range of concentration of PTX and time compared to free PTX. This kind of nanoscale drug delivery system based on PEGylated GO may find widespread application in biomedicine.

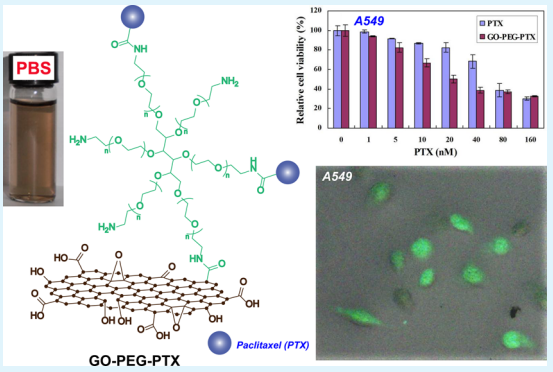

KEYWORDS: *paclitaxel, graphene oxide, PEG, drug delivery*

INTRODUCTION

Cancer has already clearly constructed a serious threat to human life and health, which could result in about 8 million new cancer patients, and more than 6 million people die of it in the world every year. Therefore, studying antitumor drugs is one of the hot topics at present. Around the world, about 80 kinds of antitumor drugs were used in clinical treatment, such as camptothecin (CPT), paclitaxel (PTX), doxorubicin hydrochloride (DOX), and so on.[1,2] Among them, PTX is a commonly used potent chemotherapeutic agent which shows high cytotoxicity to cancer cells.[3] PTX was first derived from the bark of Western Yew tree in 1963, while its chemical structure was definitely confined until 1971.[4] During clinical trails, PTX has demonstrated significant activity against a wide variety of tumors, including refractory ovarian cancer, metastatic breast cancer, nonsmall cell lung cancer, AIDS-related Kaposi's sarcoma, head and neck malignancies, and other cancers.[3,5,6] PTX has been considered as the most significant progress in tumor chemotherapy in recent decades by the National Cancer Institute (NCI).[7] In 1992, Bristol-Myers Squibb Co. marketed this drug as TAXOL with the approval of the Food and Drug Administration (FDA), where it was employed for treatment of breast, ovary, and AIDS-related Kaposi sarcoma.[8]

However, low water solubility, poor bioavailability, and emergence of drug resistance in patients limited the biological application of PTX.[9,10] Presently, the only preparation used in clinical therapy was prepared by dehydrated alcohol (1:1, v/v) with cremophor EL as cosolvent, and it must be further diluted with 0.9% sodium chloride injection prior to use, while cremophor EL has significant toxic side effects.[11,12] In previous reports, some researchers have employed drug delivery systems to improve the utilization and reduce the side effects of PTX. Kim et al. synthesized a biodegradable amphiphilic diblock copolymer, monomethoxy poly(ethylene glycol)-*block*-poly(D,L-lactide) (mPEG-PDLLA), to load PTX, and they found the polymeric micellar paclitaxel formulation showed advantages over commercially available injectable preparation of paclitaxel in terms of low toxicity levels and increased dose after injected to mice.[13] Fonseca et al. reported the preparation of paclitaxel-loaded PLGA nanoparticles, and the nanoparticles

Received: November 10, 2014
Accepted: December 29, 2014
Published: December 29, 2014

DOI: 10.1021/am507798d
ACS Appl. Mater. Interfaces 2015, 7, 1355−1363

Scheme 1. Preparation of GO-PEG-PTX Nanoscale Drug Delivery System

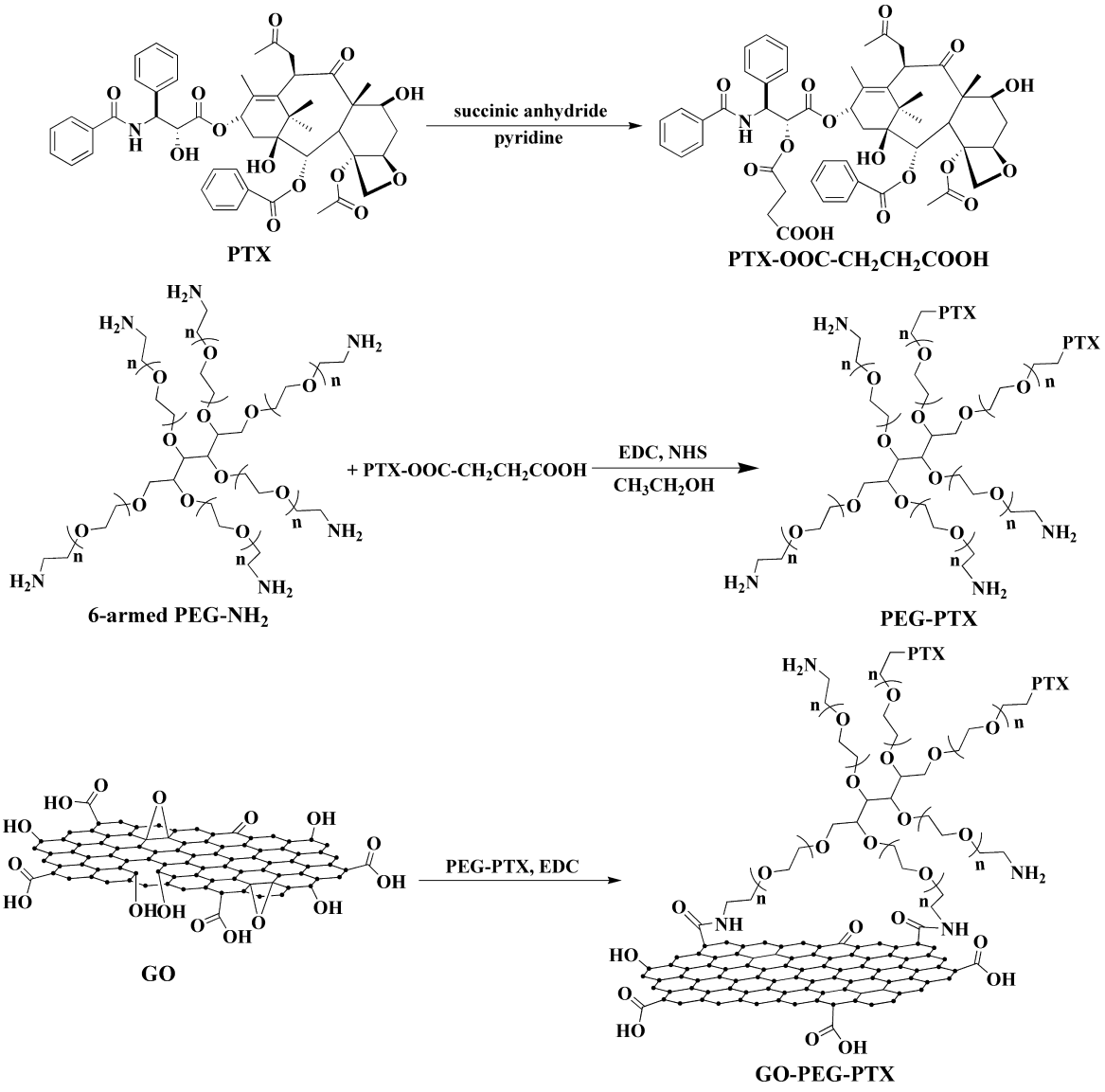

exhibited high incorporation efficiencies of PTX which strongly enhanced its antitumoral efficacy more than the free drug.[14]

In comparison with other drug carriers, graphene oxide (GO), the oxidation derivative of graphene, has recently attracted significant attention in many areas, especially in biological application.[15−21] After oxidation, hydrophilic groups such as hydroxyl, carboxyl, and epoxy groups can be introduced onto the basal planes and edges of GO sheets, which provide better dispersibility in pure water and also offer reactive sites for further functionalization via specific interactions.[22−24] However, GO will aggregate in solutions rich in salts or proteins such as cell medium and serum.[24] In order to improve its biocompatibility and physiological stability, some micromolecule and polymer was introduced onto GO. For instance, Zhang et al. functionalized GO with sulfonic acid groups, which rendered GO stable in physiological solution. Furthermore, after loading DOX and CPT via $\pi-\pi$ stacking and hydrophobic interactions, the nanocarrier exhibited high cytotoxicity to MCF-7 cells.[25] Among the commercially available polymers, poly(ethylene glycol) (PEG) is a very useful reagent in biology because of its minimal toxicity, biocompatibility, protein resistance, and good solubility in water or other common solvents.[26−30]

In the current work, we proposed a new GO-based drug delivery system (Scheme 1) to improve the utilization rate of PTX for cancer therapy. We first chemically modified PTX with succinic anhydride to convert a hydroxyl to carboxyl, and then the modified PTX was connected to biocompatible 6-armed starlike PEG, giving the PTX-terminated PEG, PEG-PTX.[31] In the following step, we functionalized GO through grafting PEG-PTX onto the surface of GO sheets for affording the target nanoscale drug delivery system, GO-PEG-PTX. The successful preparation of GO-PEG-PTX was confirmed by UV−vis spectroscopy, atomic force microscopy (AFM), and thermogravimetric analysis (TGA). Moreover, fluorescein isothiocyanate (FITC) was linked to GO-PEG to provide an analog of GO-PEG-PTX, GO-PEG-FITC as shown in Scheme 2, for investigating the cellular uptake behavior. GO-PEG-FITC could be efficiently taken up by A549 lung cancer cells and MCF-7 breast cancer cells in a short time as evidenced by the intracellular imaging. It was demonstrated that GO-PEG-PTX could be a highly potent killer of cancer cells in vitro with a

DOI: 10.1021/am507798d
ACS Appl. Mater. Interfaces 2015, 7, 1355−1363

Scheme 2. Synthetic Route of GO-PEG-FITC

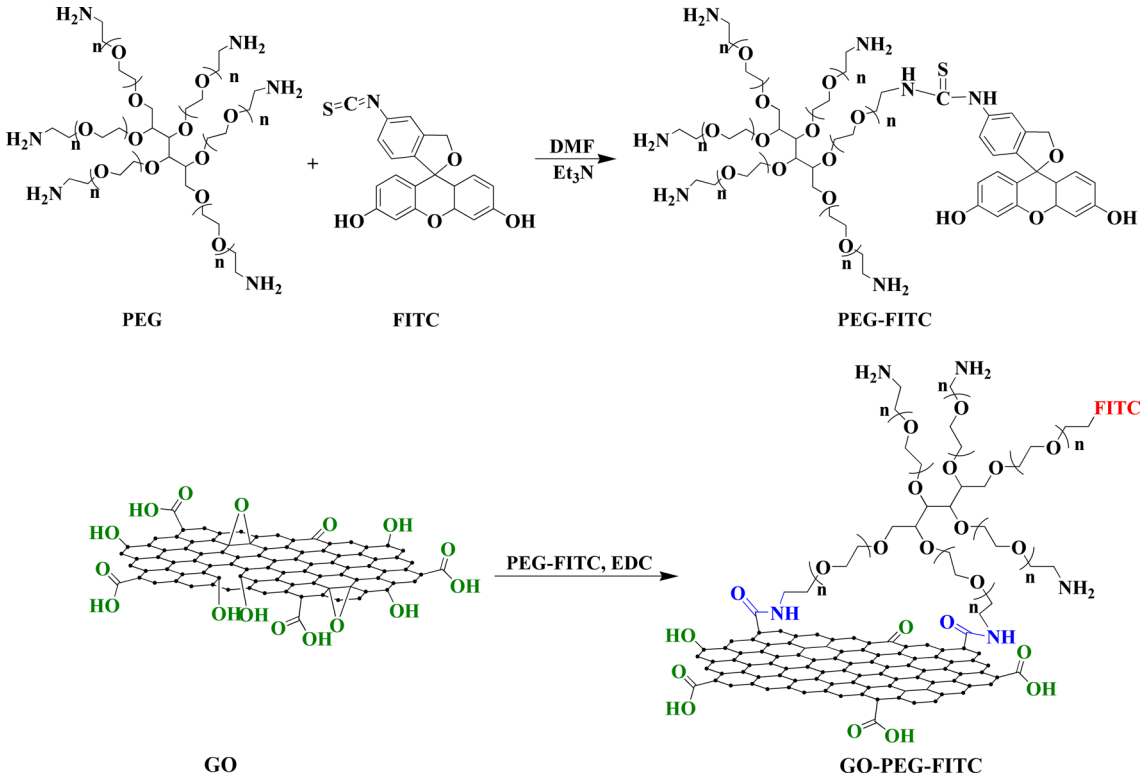

higher cytotoxicity to A549 and MCF-7 cells compared to free PTX from the cell viability assay. This way could significantly improve the bioavailability of PTX as well as other hydrophobic drugs.

EXPERIMENTAL SECTION

Materials. Six-armed PEG with six hydroxyl end groups (6-armed PEG−OH, M_n = 5300 g/mol determined by MALDI-TOF-MS, M_w/M_n = 1.04 determined by GPC) was synthesized by anionic polymerization of ethylene oxide using D-mannitol as initiator.[32] Graphite powder (Aldrich, 99.99+%), fluorescein isothiocyanate (FITC, Aldrich, 90%), paclitaxel (PTX, Aldrich, 99%), sulfuric acid (H_2SO_4, Aldrich, 95−98%), sodium nitrate ($NaNO_3$, Aldrich, 99%), *N*-(3-(dimethylamino)propyl)-*N*′-ethylcarbodiimide hydrochloride (EDC·HCl, Aldrich, 99%), potassium permanganate ($KMnO_4$, Aldrich, 99%), succinic anhydride (Aldrich, 97%), *N*,*N*-dimethylformamide (DMF, Aldrich, 99.8%), pyridine (Aldrich, 99%), and cell counting kit-8 (CCK-8, Dojindo, Japan) were used as received. RPMI 1640 and DMEM medium were purchased from GIBCO/Invitrogen, USA, and supplemented with 10% fetal bovine serum (FBS, BI Biological Industries Ltd., Israel) and 1% penicillin−streptomycin (10 000 U/mL penicillin and 10 mg/mL streptomycin, Solarbio Life Science, China). Six-armed PEG−OH was converted to 6-armed PEG with six amino end groups, 6-armed PEG−NH_2, according to a previous report.[33]

Measurements. ^{1}H NMR (500 MHz) analyses were performed on a Bruker Avance 500 spectrometer; tetramethylsilicane was used as internal standard. UV−vis spectra were measured by a Hitachi U-2910 spectrophotometer. Absolute number-average molecular weight was determined by MALDI-TOF-MS using an Applied Biosystems Voyager DE-STR spectrometer. Molecular weight distribution was measured by a conventional gel permeation chromatography (GPC) system equipped with a Waters 1515 Isocratic HPLC pump, a Waters 2414 refractive index detector, and a set of Waters Styragel columns (HR3 (500−30 000), HR4 (5000−600 000), and HR5 (50 000−4 000 000), 7.8 × 300 mm, particle size 5 μm). GPC measurement was carried out at 35 °C using THF as eluent (flow rate 1.0 mL/min). Atomic force microscopy (AFM) images were taken by a Veeco DI MultiMode SPM in tapping mode of dropping the sample solution onto the freshly exfoliated mica substrate. Thermogravimetry analysis (TGA) measurements were run on a TA Q500 system under N_2 purge with a heating rate of 10 °C/min. The relative cell viability was measured at the absorbance of 450 nm using a Tecan GENios Pro microplate reader. Cellular uptake images were taken by an Olympus BX51 fluorescence microscope. GO was prepared from graphite powder using neat H_2SO_4 and $KMnO_4$ according to a modified Hummer's method.[34]

Preparation of GO-PEG. GO was first dispersed in double-distilled water followed by adding 6-armed PEG−NH_2 and EDC·HCl for sonication at room temperature for 1 h. The solution was kept stirring vigorously at room temperature overnight. The final product, GO-PEG, was obtained by purifying the crude product by dialysis (MW cutoff = 14 kDa) against double-distilled water for 1 week to remove unbound 6-armed PEG−NH_2.

Preparation of GO-PEG-FITC. Six-armed PEG−NH_2 (116 mg, 0.131 mmol of −NH_2) and FITC (21 mg, 0.054 mmol) were dissolved in 15 mL of DMF, and the solution was kept stirring vigorously at room temperature for 24 h in the dark. The mixture was then dialyzed (MW cutoff = 3.5 kDa) against double-distilled water in the dark for 1 week to remove unbound FITC and DMF. PEG-FITC was obtained by freeze drying. GO-PEG-FITC was prepared by treating GO with PEG-FITC, which was the same as the preparation of GO-PEG.

Preparation of GO-PEG-PTX. PTX was first modified to PTX-COOH by transforming a hydroxyl into a carboxyl (Scheme 1) according to previous literature.[35] Six-armed PEG−NH_2 and PTX-COOH were dissolved in ethanol followed by adding EDC·HCl for sonication at room temperature. After stirring at room temperature for 10 h, the solution was dialyzed (MW cutoff = 3.5 kDa) against double-distilled water for 1 week to remove unbound PTX-COOH and ethanol. PEG-PTX was obtained by freeze drying. GO-PEG-PTX was prepared by treating GO with PEG-PTX, which was the same as the preparation of GO-PEG.

Cell Culture. Human lung cancer A549 and human breast cancer MCF-7 cells were supplied by Shanghai Institute of Cell Biology, Chinese Academy of Sciences. They were cultured at 37 °C under a

DOI: 10.1021/am507798d
ACS Appl. Mater. Interfaces 2015, 7, 1355−1363

humid 5% CO_2 atmosphere in RPMI 1640 and DMEM medium, respectively, supplemented with 10% FBS and 1% penicillin–streptomycin.

Cellular Uptake of GO-PEG-FITC. A-549 and MCF-7 cells were plated on a 20 mm glass round coverslip in 6-well plates and allowed to adhere overnight. A549 and MCF-7 cells were incubated with GO-PEG-FITC for 3 h and washed with PBS three times. The cells were then fixed in 4% paraformaldehyde at 4 °C for 30 min and stained with DAPI (2 μg/mL), a DNA-specific fluorescent dye, at 37 °C for 10 min. The stained cells were imaged under an inverted Olympus BX51 fluorescence microscope.

In Vitro Cell Viability Assay. Human lung cancer A549 and human breast cancer MCF-7 cells were plated in 96-well plates at a density of 5×10^3 cells per well in 100 μL of culture medium (RPMI 1640 for A549 and DMEM for MCF-7) and added with desired concentrations of GO-PEG, GO-PEG-PTX, and free PTX (dissolved in DMSO and diluted in PBS). The relative cell viability was measured by WST assay using CCK-8. After continuous incubation for 12, 24, 36, 48, 60, and 72 h, absorbance was measured at 450 nm using a Tecan GENios Pro microplate reader.

Statistical Analysis. Values were expressed as means ± standard deviations. Statistical analysis was performed using the Student's t test. Values of $p < 0.05$ were considered to be statistically significant.

RESULTS AND DISCUSSION

Preparation and Characterization of GO-PEG-FITC. In the present work, we designed a nanoscale drug delivery system, GO-PEG-PTX, for improving the utilization rate of PTX for cancer therapy. Apparently, in this system, PEGylated GO is used as a nanosized carrier for the delivery of PTX since that well-functionalized GO covered with biocompatible polymers such as PEG has been proved to be not obviously toxic in vitro and in vivo at the tested doses.[16,17] Then, a question of whether PEGylated GO nanocarrier (GO-PEG) could easily enter cells naturally emerged in the starting step of current study. Herein, intracellular imaging using FITC as fluorescent probe was employed to confirm whether GO-PEG carrier could readily enter cells.

The analog of GO-PEG-PTX, GO-PEG-FITC, was prepared at room temperature in two steps (Scheme 2). First, PEG-FITC was prepared by mixing FITC and 6-armed PEG-NH_2 in the presence of Et_3N, and it was characterized by ^{1}H NMR as shown in Figure 1. The characteristic proton resonance signals of FITC between 6.5 and 8.1 ppm (Figure 1A) appeared in Figure 1B after reacting with 6-armed PEG–NH_2 while the strong peak around 3.50 ppm belonged to the typical signal of 4 protons of the $-OCH_2CH_2$ repeating unit in PEG segment. In the second step, EDC·HCl was utilized as carboxyl activating regent to initiate the formation of amide linkage between GO and PEG-FITC. The unbound PEG-FITC was removed by dialysis (MW cutoff = 14 kDa) against double-distilled water for 1 week. Figure 2 shows UV–vis absorbance spectra of GO, FITC, 6-armed PEG–NH_2, PEG-FITC, and GO-PEG-FITC. GO and 6-armed PEG-NH_2 did not show any distinct absorbance peak in the range of 200–800 nm. However, after the reaction with FITC, the spectrum of the resulting product, i.e., PEG-FITC, showed a strong absorption peak near 488 nm originating from FITC; this result combined with ^{1}H NMR spectrum in Figure 1B clearly verified the successful binding of FITC to PEG. Similarly, the broad weak absorption peak near 488 nm in UV–vis absorbance spectrum of the resultant after treating GO with PEG-FITC demonstrated the successful preparation of FITC-labeled GO-PEG nanocomplex, GO-PEG-FITC.

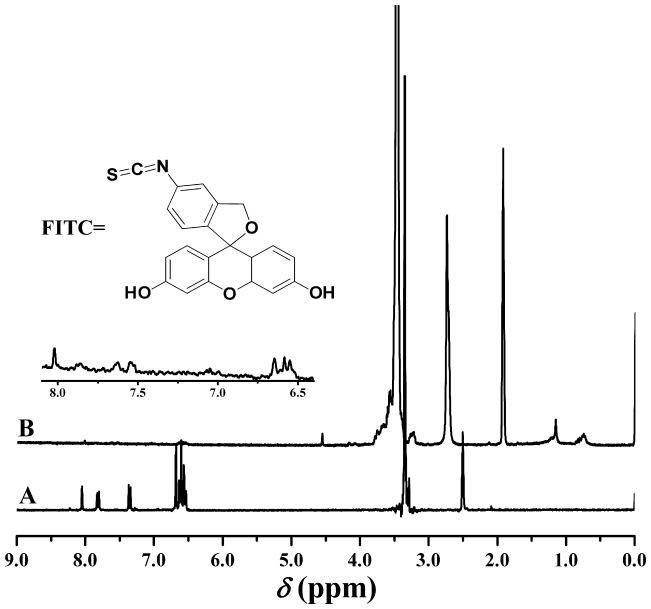

Figure 1. ^{1}H NMR spectra of FITC in DMSO-d_6 (A) and PEG-FITC in acetone-d_6 (B); (inset) enlarged region of δ = 6.5–8.0 ppm of the spectrum of PEG–PITC.

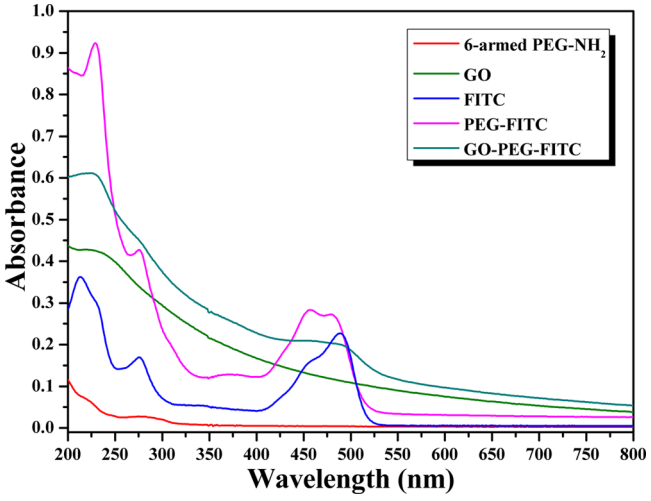

Figure 2. UV–vis absorbance spectra of GO, FITC, 6-armed PEG–NH_2, PEG-FITC, and GO-PEG-FITC in aqueous solution.

Cellular Uptake and Cytotoxicity of Nanocarrier. The cellular uptake of GO-PEG-FITC with FITC as a fluorescent probe was then investigated by incubating human lung cancer A549 and human breast cancer MCF-7 cells with GO-PEG-FITC for intracellular fluorescence imaging.[36] We can clearly observe the fluorescence in both A549 and MCF-7 cells only after incubating for a short time of 3 h (Figure 3). In comparison with the nuclei staining of DAPI, the localization of FITC was both in the cytoplasm and in the nucleus. This fact definitely illustrated that PEGylated GO nanocarrier, GO-PEG, could easily penetrate the cell membranes and quickly enter A549 and MCF-7 cells. Thus, we can confirm the cellular uptake of GO-PEG by A549 and MCF-7 cells.

Next, WST-8-based colorimetric assay was used to examine the cytotoxicity of GO-PEG nanocarrier on A549 and MCF-7 cells so as to verify whether GO-PEG nanocarrier is nontoxic to A549 and MCF-7 cells. A549 and MCF-7 cells were first

DOI: 10.1021/am507798d
ACS Appl. Mater. Interfaces 2015, 7, 1355–1363

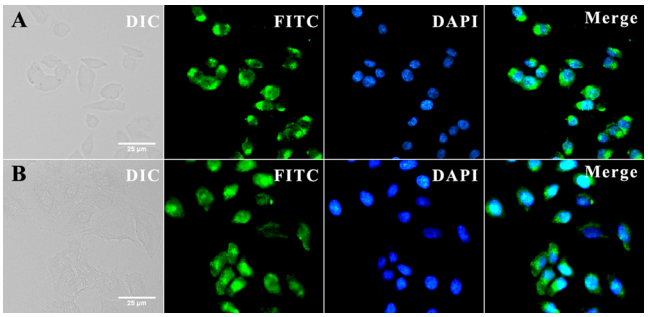

Figure 3. Differential interference contrast (DIC), FITC, DAPI, and merge (FITC+DAPI) images of A549 (A) and MCF-7 (B) cells incubated with GO-PEG-FITC for 3 h; scale bar 25 μm.

incubated in the suitable mediums of RPMI 1640 and DMEM containing various concentrations of GO-PEG, respectively. It can be seen from Figure 4 that high cell viabilities (>92%) were detected for both A549 and MCF-7 cells with various concentrations of GO-PEG even after incubating for a long tome of 72 h, even at a high concentration up to 200 mg/L. These aforementioned results clearly demonstrated that GO-PEG nanocarrier indeed was not cytotoxic by itself.

Preparation and Characterization of GO-PEG-PTX. The synthetic route for the preparation of GO-PEG-PTX nanoscale drug delivery system is shown in Scheme 1. The chemotherapy drug, PTX, was first modified by converting the hydroxyl at the 2′ position to the carboxyl using succinic anhydride without affecting the chemotherapy effect,[35] obviously enhancing the reactivity (−COOH vs −OH) with 6-armed PEG−NH_2. Conjugation of carboxyl-functionalized PTX with 6-armed PEG-NH_2, i.e., PEG−PTX, through the formation of an amide bonding by the reaction between amino groups of 6-armed PEG-NH_2 and carboxyl of modified PTX was evidenced by ^{1}H NMR. For pure PTX, no resonance signal appeared between 2.60 and 2.70 ppm (Figure 5A), while for carboxyl-functionalized PTX, two characteristic peaks at 2.63 (a) and 2.70 (b) ppm corresponding to the protons of succinic anhydride were clearly distinguished in Figure 5B. In Figure 5C, a series of typical peaks of PTX in the range of 0−9 ppm and a strong

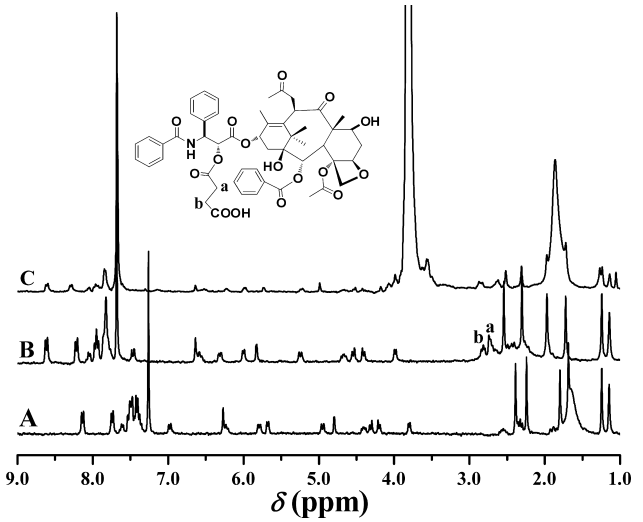

Figure 5. ^{1}H NMR spectra of PTX (A), carboxyl-functionalized PTX (B), and PEG-PTX (C) in $CDCl_3$.

peak around 3.60 ppm originating from PEG proved the successful preparation of PEG-PTX.

In the following step, GO-PEG-PTX was prepared using the same method by treating the remaining amino groups in the terminal of PEG segment of PEG-PTX with carboxyls on the surface of GO sheets in the presence of EDC·HCl. The pure product, GO-PEG-PTX, was obtained by removing the unbound PEG-PTX through dialysis. The successful binding of PEG-PTX on GO sheets was affirmed by the characteristic absorption peak at 229 nm originating from PTX in UV−vis absorbance spectrum after the reaction between GO and PEG-PTX (Figure 6), which was absent in that before conjugation. Moreover, the binding capacity (weight ratio of bound PTX to PEG), i.e., the weight percentage of PTX in PEG-PTX, was estimated to be 11.2 wt % via the standard absorption curve of PTX at 229 nm. Therefore, the drug loading ratio, i.e., the weight percentage of PTX in GO-PEG-PTX, could be estimated via multiplying the weight percentage of PEG-PTX in GO-PEG-PTX by the weight percentage of PTX in PEG-PTX (11.2 wt %), which would be described in the latter part.

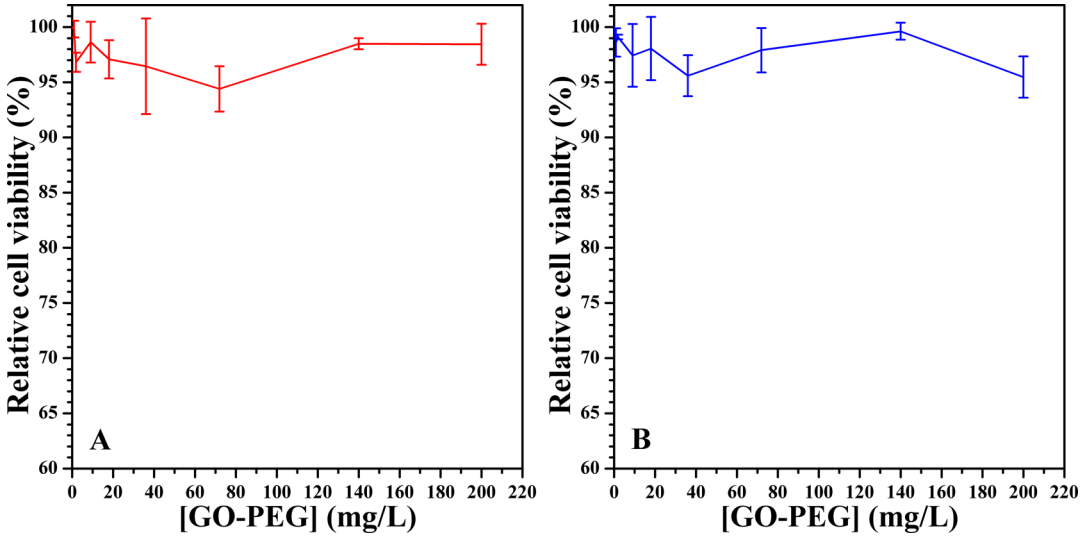

Figure 4. Relative cell viability of A549 (A) and MCF-7 (B) cells after 72 h incubation with GO-PEG; error bars were based on triplet samples.

DOI: 10.1021/am507798d
ACS Appl. Mater. Interfaces 2015, 7, 1355−1363

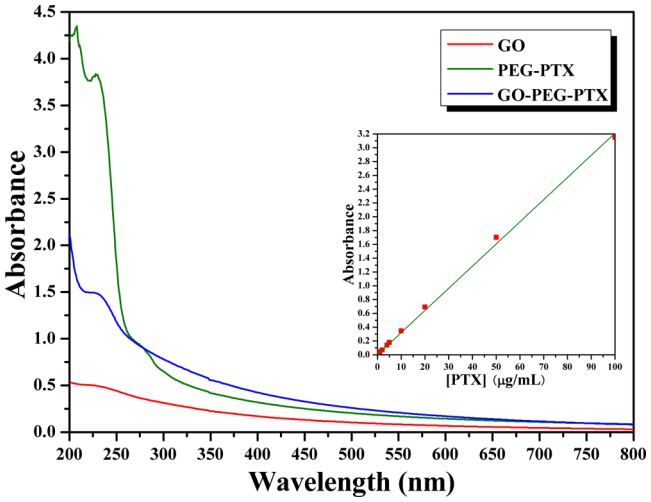

Figure 6. UV−vis absorbance spectra of GO (0.015 mg/mL), PEG-PTX (1.0 mg/mL), and GO-PEG-PTX (0.1 mg/mL) in aqueous solution; (inset) UV−vis absorbance standard curve of PTX at 229 nm.

Figure 7A shows the morphology of GO-PEG-PTX visualized by AFM. It was found that GO-PEG-PTX possessed a rough surface with some protuberances in comparison with the reported smooth surface of GO sheets,[24] mainly due to the attachment of PEG-PTX onto both planes of GO sheets. The thickness of GO-PEG-PTX sheets was measured to be at 1.7−3.8 nm higher than that of GO.[24] GO-PEG-PTX were stable in water, PBS, and RPMI 1640 solutions even after 30 days without any precipitation as shown in Figure 7B, while GO quickly aggregated and precipitated in PBS and RPMI 1640 solutions. GO-PEG-PTX sheets had a lateral size between 50 and 200 nm as shown in Figure 7C; this size could greatly benefit the application for drug delivery because of the well-known enhanced permeability and retention (EPR) effect.[37] Thus, the dimension of GO-PEG-PTX was very suitable for drug delivery.

In order to determine the content of PEG-PTX attached onto GO sheets, TGA was used to measure the thermal stabilities of GO, PEG-PTX, and GO-PEG-PTX in N_2. As shown in Figure 8, the mass loss of GO started below 100 °C because of the volatilization of stored water in the π-stacked structure,[34] which meant that GO was thermally unstable. The mass loss was obviously accelerated in the range of 170−230

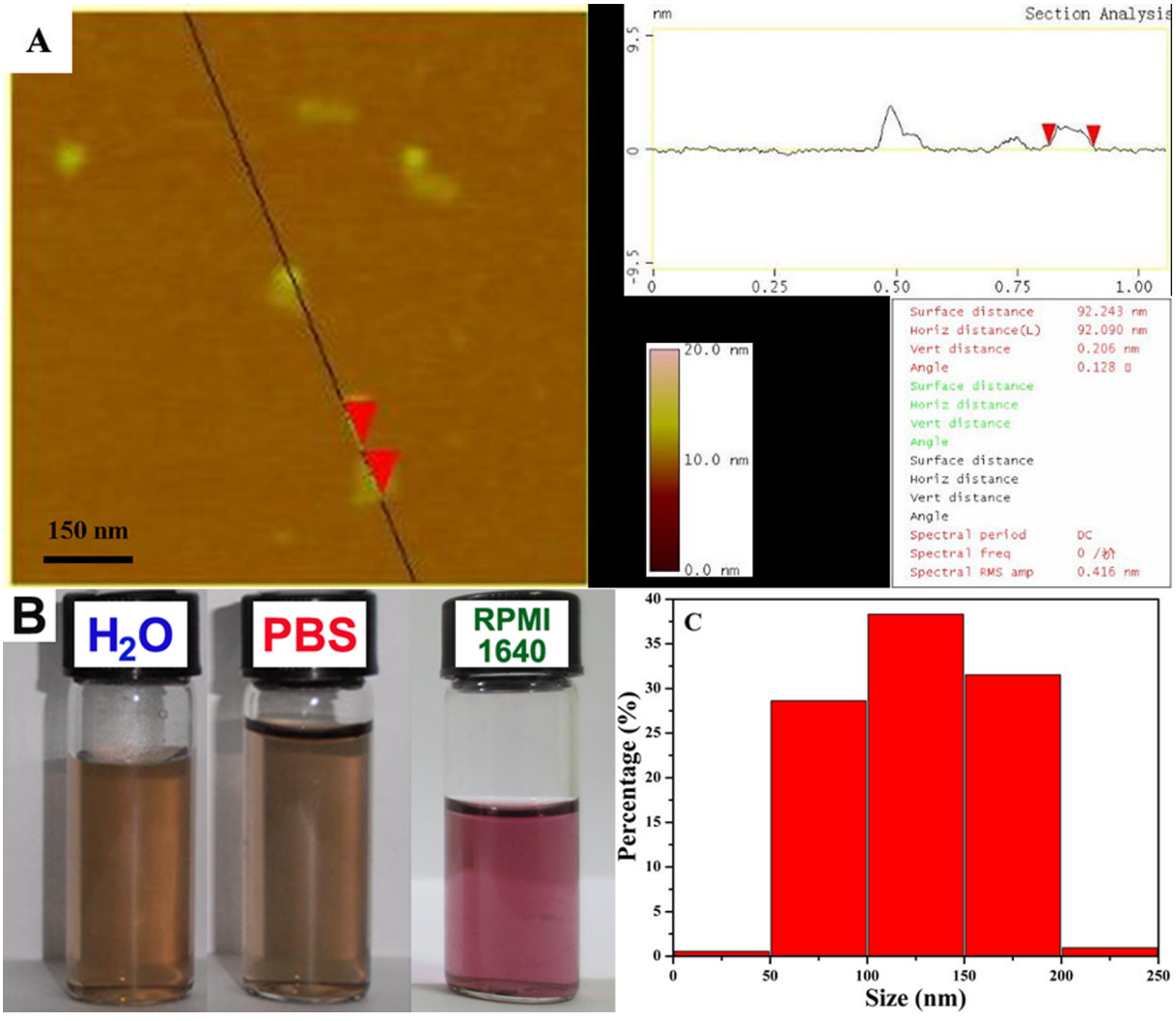

Figure 7. AFM image of GO-PEG-PTX (A), in vitro stability of GO-PEG-PTX in water, PBS, and RPMI 1640 solutions after placing 30 days (B), and size statistical graph (C).

DOI: 10.1021/am507798d
ACS Appl. Mater. Interfaces 2015, 7, 1355−1363

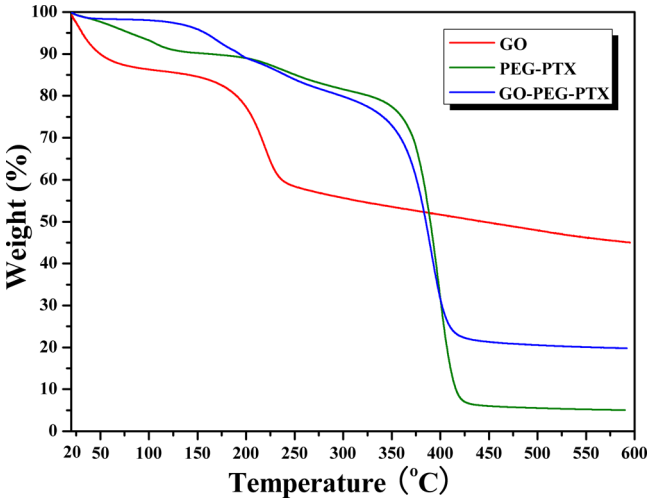

Figure 8. TGA (in N_2) of GO, PEG-PTX, and GO-PEG-PTX with a heating rate of 10 °C/min.

°C due to the pyrolysis of labile oxygen-containing groups.[34] After GO was linked with PEG-PTX, the mass loss of the resultant GO-PEG-PTX was remarkably accelerated from 350 °C, which was nearly 180 °C higher than that of GO. This point clearly indicated that the polymeric coating was very efficacious for increasing the thermal stability of GO sheets. The weight loss of GO-PEG-PTX at 600 °C in N_2 was 80.2%, while GO and PEG-PTX had a 55.0% and 95.0% weight loss at 600 °C in N_2, respectively. Thus, GO-PEG-PTX was evaluated to contain about 37 wt % of GO and 63 wt % of PEG-PTX according to the following equation set (x and y are the weight percentage of GO and PEG-PTX, respectively).

$$0.55x + 0.95y = 0.802 \quad (1)$$

$$x + y = 1 \quad (2)$$

Combining the weight percentage of PTX in PEG-PTX (11.2 wt %) obtained from UV−vis spectroscopy, we could calculate the drug loading ratio, i.e., the weight percentage of PTX in GO-PEG-PTX via multiplying the weight percentage of PTX in PEG-PTX (11.2 wt %) by the content of PEG-PTX in GO-PEG-PTX (63 wt %), and the drug loading ratio was approximately 7.1 wt %.

In Vitro Cell Toxicity of GO-PEG-PTX. In the current work, WST-8-based colorimetric assay was utilized to examine the cytotoxicity effects of GO-PEG-PTX nanoscale system and free PTX on A549 and MCF-7 cells. A549 and MCF-7 cells were first incubated with free PTX and GO-PEG-PTX for 72 h with varying the concentration of PTX from 0 to 160 nM, and their relative cell viabilities are shown in Figure 9A and 9B, respectively. Both free PTX and GO-PEG-PTX were found to inhibit A549 and MCF-7 cells in a time-dependent manner, and the relative cell viability declined monotonously with ascending the concentration of PTX. When the concentration of PTX was very low (≤1 nM), both GO-PEG-PTX and free PTX had similar cytotoxicity effects on both A549 and MCF-7 cells; the cell viabilities were all higher than 91% with very small margins below 5%. Nevertheless, GO-PEG-PTX obviously showed a higher cytotoxic effect on both cells in comparison with free PTX with raising the concentration of PTX. For example, the viabilities of A549 cell were 82.5% for free PTX and 50.1% for GO-PEG-PTX with a settled PTX concentration of 20 nM,

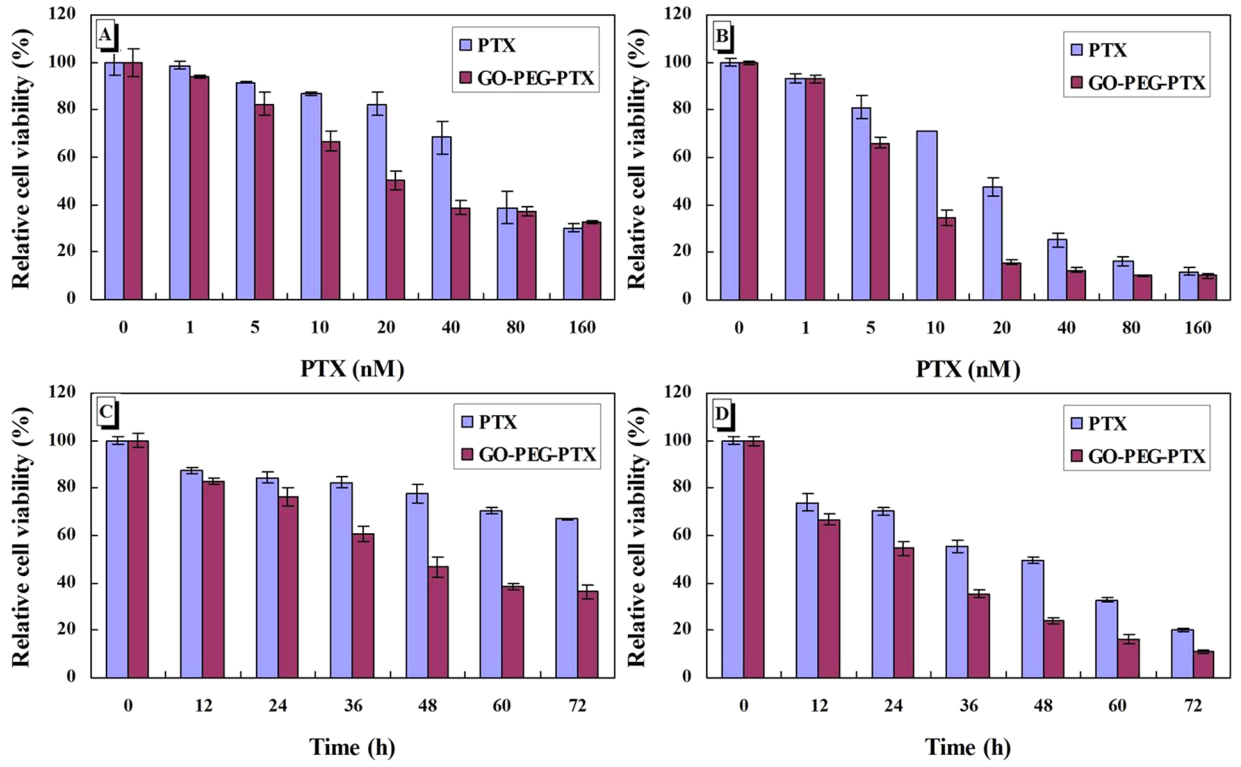

Figure 9. Relative cell viability of cells after treatment with different concentrations of PTX and GO-PEG-PTX for 72 h ((A) A-549 and (B) MCF-7) and with different time at a constant PTX concentration of 40 nM ((C) A-549 and (D) MCF-7). Experiments were repeated three times, all with similar results. Data are presented as the mean ± SD (for each group, n = 3).

DOI: 10.1021/am507798d
ACS Appl. Mater. Interfaces 2015, 7, 1355−1363

respectively; meanwhile, the viabilities of MCF-7 cell were 47.7% for free PTX and 15.8% for GO-PEG-PTX with a certain PTX concentration of 20 nM. Because MCF-7 cell was much sensitive to PTX than the A549 cell, it exhibited a higher cytotoxicity effect than the A549 cell with the same concentration of PTX at a comparable incubation time. When the concentration of PTX was increased above 80 nM, the disparity of relative cell viability after incubating with free PTX and GO-PEG-PTX apparently decreased because of the drastic toxicity of drug to cells at high concentrations. Furthermore, it was worthy pointing out that GO-PEG-PTX with a low concentration of PTX exhibited a high cytotoxicity similar to free PTX with a high concentration. For instance, the viability of the A549 cell was 38.6% for free PTX with a concentration of 80 nM, while it was 38.6% for GO-PEG-PTX with just 40 nM of PTX; the viability of the MCF-7 cell was 16.4% for free PTX with a concentration of 80 nM, while it was 15.8% for GO-PEG-PTX with only 20 nM of PTX. These results clearly indicated that GO-PEG nanocarrier could be used to load a low concentration of PTX for achieving the same treatment using a higher concentration of free PTX, i.e., GO-PEG nanocarrier could improve the drug efficacy of PTX without increasing the dose of PTX.

In addition, the effect of incubation time (12−72 h) on the cytotoxicity of GO-PEG-PTX and free PTX with a fixed concentration of PTX (40 nM) was investigated. It can be seen from Figure 9C and 9D that A549 and MCF-7 cells were inhibited by both free PTX and GO-PEG-PTX in a time-dependent mode. GO-PEG-PTX obviously exhibited a higher cytotoxicity effect on A549 and MCF-7 cells originating from the enhanced PTX cellular uptake in comparison with free PTX at every time point. Besides, GO-PEG-PTX showed similar cytotoxicity compared to that of free PTX at shorter incubation time. The viability of A549 cell after incubating with free PTX for 72 h was 66.9%; however, it only took GO-PEG-PTX 36 h to reach this value (60.8%), and the cell viability was as low as 36.3% after 72 h, which was much lower than that of free PTX; the viability of MCF-7 cell after incubating with free PTX for 72 h was 20.3%, while GO-PEG-PTX only spent 48 h to get close to this value (24.0%), and the cell viability was as low as 10.9% after 72 h, which was much lower than that of free PTX. These above-mentioned results indicated that GO-PEG nanocarrier could load PTX to attain a quicker treatment in comparison with that of free PTX so as for improving the efficacy of PTX.

CONCLUSIONS

In summary, we reported the synthesis of PEGylated GO with good biocompatibility and physiological stability and its application as a nanocarrier to deliver a water-insoluble anticancer drug of PTX. Fluorescence observation demonstrated that GO-PEG-conjugated FITC can quickly enter A549 and MCF-7 cells. GO-PEG nanocarrier was proved to be practically nontoxic, and the GO-PEG-PTX nanocomplex was found to be potent against cancer cells, killing in vitro as evaluated by WST-8 assay. It was illustrated that GO-PEG-PTX inhibited A549 and MCF-7 cells in a concentration- and time-dependent manner, and it exhibited a higher cytotoxicity effect compared to free PTX, especially at lower concentration and shorter time, for improving the bioavailability of PTX. On the basis of aforementioned results, PEG-functionalized GO, GO-PEG, could be a promising nanomaterial in biological and medical areas.

AUTHOR INFORMATION

Corresponding Authors

*E-mail: ship@ecust.edu.cn.
*E-mail: xyhuang@mail.sioc.ac.cn.

Notes

The authors declare no competing financial interest.

ACKNOWLEDGMENTS

The authors are thankful for financial support from the National Natural Science Foundation of China (21204098, 31100549, and 11275050), Shanghai Scientific and Technological Innovation Project (11 nm0501100, 11ZR1445900, 14520720100, and 14520720700), State Key Laboratory of Bioreactor Engineering (2060204), and Fundamental Research Funds for the Central Universities (222201313010). We thank Prof. Guowei Wang (Fudan Univeristy) for assistance in synthesizing 6-armed PEG.

REFERENCES

(1) Yang, X. Y.; Zhang, X. Y.; Liu, Z. F.; Ma, Y. F.; Huang, Y.; Chen, Y. S. High-Efficiency Loading and Controlled Release of Doxorubicin Hydrochloride on Graphene Oxide. *J. Phys. Chem. C* **2008**, *112*, 17554−17558.

(2) Johnson, J. A.; Lu, Y. A.; Burts, A. O.; Xia, Y.; Durrell, A. C.; Tirrell, D. A.; Grubbs, R. H. Drug-Loaded, Bivalent-Bottle-Brush Polymers by Graft-Through ROMP. *Macromolecules* **2010**, *43*, 10326−10335.

(3) Huizing, M. T.; Misser, V. H.; Pieters, R. C.; ten Bokkel Huinink, W. W.; Veenhof, C. H.; Vermorken, J. B.; Pinedo, H. N.; Beijnen, J. H. Taxanes: A New Class of Antitumor Agents. *Cancer Invest.* **1995**, *13*, 381−404.

(4) Wani, M. C.; Taylor, H. L; Wall, M. E.; Coggon, P.; McPhail, A. P. Plant Antitumour Agents. VI. Isolation and Structure of Taxol, A Novel Antileukemic and Antitumor Agent from Taxus Brevioflia. *J. Am. Chem. Soc.* **1971**, *93*, 2325−2327.

(5) Rowinsky, E. K.; Cazenave, L. A.; Donehower, R. C. Taxol: A Novel Investigational Antimicrotubule Agent. *J. Natl. Cancer Inst.* **1990**, *82*, 1247−1259.

(6) Wall, E. M.; Wan, M. C. Camptothecin and Taxol: Discovery to Clinic. *Cancer Res.* **1995**, *55*, 753−760.

(7) Smith, D. C.; Chay, C. H.; Dunn, R. L.; Fardig, J.; Esper, P.; Olson, K. Phase II Trial of Paclitaxel, Estramustine, Etoposide, and Carboplatin in the Treatment of Patients with Hormone-Refractory Prostate Carcinoma. *Cancer* **2003**, *98*, 269−276.

(8) Nilufer, J. S. F.; Dong, Z.; Wang, Y. L. Taxanes: Promising Anti-Cancer Drugs. *Asian Pac. J. Cancer Prev.* **2011**, *12*, 837−851.

(9) Singla, A. K.; Garg, A.; Aggarwal, D. Paclitaxel and Its Formulations. *Int. J. Pharm.* **2002**, *235*, 179−192.

(10) Jin, J. Y.; Lee, W. S.; Joo, K. M.; Maiti, K. K.; Biswas, G.; Kim, W.; Kim, K. T.; Lee, S. J.; Kim, K. H.; Nam, D. H.; Chung, S. K. Preparation of Blood-Brain Barrier-Permeable Paclitaxel-Carrier Conjugate and Its Chemotherapeutic Activity in the Mouse Glioblastoma Model. *Med. Chem. Commun.* **2011**, *2*, 270−273.

(11) Goldspiel, B. R. Pharmaceutical Issues: Preparation, Administration, Stability, and Compatibility with Other Medications. *Ann. Pharmacother.* **1994**, *28*, s23−s26.

(12) Weiss, R. B.; Donehower, R. C.; Wiernik, P. H.; Ohnuma, T.; Gralla, R. J.; Trump, D. L.; Baker, J. R.; VanEcho, D. A.; VonHoff, D. D.; Leyland-Jones, B. Hypersensitivity Reactions from Taxol. *J. Clin. Oncol.* **1990**, *8*, 1263−1268.

(13) Kim, S. C.; Kim, D. W.; Shim, Y. H.; Bang, J. S.; Oh, H. S.; Kim, S. W.; Seo, M. H. *In vivo* Evaluation of Polymeric Micellar Paclitaxel Formulation: Toxicity and Efficacy. *J. Controlled Release* **2001**, *72*, 191−202.

DOI: 10.1021/am507798d
ACS Appl. Mater. Interfaces 2015, 7, 1355−1363

(14) Fonseca, C.; Simoes, S.; Gaspar, R. Paclitaxel-Loaded PLGA Nanoparticles: Preparation, Physicochemical Characterization and *in vitro* Anti-Tumoral Activity. *J. Controlled Release* **2002**, *83*, 273−286.
(15) Bao, H. Q.; Pan, Y. Z.; Ping, Y.; Sahoo, N. G.; Wu, T. F.; Li, L.; Li, J.; Gan, L. H. Chitosan-Functionalized Graphene Oxide as a Nanocarrier for Drug and Gene Delivery. *Small* **2011**, *7*, 1569−1578.
(16) Yang, K.; Wan, J. M.; Zhang, S. A.; Zhang, Y. J.; Lee, S. T.; Liu, Z. *In vivo* Pharmacokinetics, Long-Term Biodistribution, and Toxicology of PEGylated Graphene in Mice. *ACS Nano* **2011**, *5*, 516−522.
(17) Zhang, Y. B.; Ali, S. F.; Dervishi, E.; Xu, Y.; Li, Z. R.; Casciano, D.; Biris, A. S. Cytotoxicity Effects of Graphene and Single-Wall Carbon Nanotubes in Neural Phaeochromocytoma-Derived PC12 Cells. *ACS Nano* **2010**, *4*, 3181−3186.
(18) Bitounis, D.; Ali-Boucetta, H.; Hong, B. H.; Min, D. H.; Kostarelos, K. Prospects and Challenges of Graphene in Biomedical Applications. *Adv. Mater.* **2013**, *25*, 2258−2268.
(19) Du, L. B.; Suo, S.; Luo, D.; Jia, H. Y.; Sha, Y. L.; Liu, Y. Hydroxyethylated Graphene Oxide as Potential Carriers for Methotrexate Delivery. *J. Nanopart. Res.* **2013**, *15*, 1708−1714.
(20) Makharza, S.; Cirillo, G.; Bachmatiuk, A.; Ibrahim, I.; Ioannides, N.; Trzebicka, B.; Hampel, S.; Rummeli, M. H. Graphene Oxide-Based Drug Delivery Vehicles: Functionalization, Characterization, and Cytotoxicity Evaluation. *J. Nanopart. Res.* **2013**, *15*, 2099−2124.
(21) Wang, Y.; Li, Z. H.; Wang, J.; Li, J. H.; Lin, Y. H. Graphene and Graphene Oxide: Biofunctionalization and Applications in Biotechnology. *Cell* **2013**, *29*, 205−212.
(22) He, H. Y.; Klinowski, J.; Forster, M.; Lerf, A. A New Structural Model for Graphite Oxide. *Chem. Phys. Lett.* **1998**, *287*, 53−56.
(23) Yang, H. F.; Shan, C. S.; Li, F. H.; Han, D. X.; Zhang, Q. X.; Niu, L. Covalent Functionalization of Polydisperse Chemically-Converted Graphene Sheets with Amine-Terminated Ionic Liquid. *Chem. Commun.* **2009**, 3880−3882.
(24) Liu, Z.; Robinson, J. T.; Sun, X. M.; Dai, H. J. PEGylated Nanographene Oxide for Delivery of Water-Insoluble Cancer Drugs. *J. Am. Chem. Soc.* **2008**, *130*, 10876−10877.
(25) Zhang, L. M.; Xia, J. G.; Zhao, Q. H.; Liu, L. W.; Zhang, Z. J. Functional Graphene Oxide as a Nanocarrier for Controlled Loading and Targeted Delivery of Mixed Anticancer Drugs. *Small* **2010**, *6*, 537−544.
(26) Prentice, D. E.; Majeed, S. K. Oral Toxicity of Polyethylene Glycol (PEG 200) in Monkeys and Rats. *Toxicol. Lett.* **1978**, *2*, 119−122.
(27) Torchilin, V. P.; Omelyanenko, V. G.; Parisov, M. I.; Bogdanov, A. A.; Trubetskoy, V. S.; Herron, J. N.; Gentry, C. A. Poly(ethylene glycol) on the Liposome Surface: on the Mechanism of Polymer-Coated Liposome Longevity. *Biochim. Biophys. Acta* **1994**, *1195*, 11−20.
(28) Zalipsky, S. Chemistry of Polyethylene Glycol Conjugates with Biologically Active Molecules. *Adv. Drug Delivery Rev.* **1995**, *16*, 157−182.
(29) Leung, H. W.; Ballantyne, B.; Hermansky, S. J.; Franta, S. W. Peroral Subchronic, Chronic Toxicity, and Pharmacokinetic Studies of a 100-Kilo Dalton Polymer of Ethylene Oxide (Polyox N-10) in the Fischer 344 Rat. *Int. J. Toxicol.* **2000**, *19*, 305−312.
(30) Yamaoka, T.; Tabata, Y.; Ikada, Y. Distribution and Tissue Uptake of Poly(ethylene glycol) with Different Molecular Weights after Intravenous Administration to Mice. *J. Pharm. Sci.* **1994**, *83*, 601−606.
(31) Magri, N. F.; Kingston, D. G. I. Modified Taxols, 4. Synthesis and Biological Activity of Taxols Modified in the Side chain. *J. Nat. Prod.* **1988**, *51*, 298−306.
(32) Rele, S. M.; Cui, W. X.; Wang, L. C.; Hou, S. J.; Barr-Zarse, G.; Tatton, D.; Gnanou, Y.; Esko, J. D.; Chaikof, E. L. Dendrimer-like PEO Glycopolymers Exhibit Anti-Inflammatory Properties. *J. Am. Chem. Soc.* **2005**, *127*, 10132−10133.
(33) Mei, B. C.; Susumu, K.; Medintz, I. L.; Delehanty, J. B.; Mountziaris, T. J.; Mattoussi, H. Modular Poly(ethylene glycol) Ligands for Biocompatible Semiconductor and Gold Nanocrystals with Extended pH and Ionic Stability. *J. Mater. Chem.* **2008**, *18*, 4949−4958.
(34) Fang, M.; Wang, K. G.; Lu, H. B.; Yang, Y. L.; Nutt, S. Covalent Polymer Functionalization of Graphene Nanosheets and Mechanical Properties of Composites. *J. Mater. Chem.* **2009**, *19*, 7098−7105.
(35) Deutsch, H. M.; Glinski, J. A.; Hernandez, M.; Haugwitqt, R. D.; Narayanan, V. L.; Suffness, M.; Zalkow, L. H. Synthesis of Congeners and Prodrugs. 3. Water- Soluble Prodrugs of Taxol with Potent Antitumor Activity. *J. Med. Chem.* **1989**, *32*, 788−792.
(36) Peng, C.; Hu, W.; Zhou, Y.; Fan, C. H.; Huang, Q. Intracellular Imaging with a Graphene-Based Fluorescent Probe. *Small* **2010**, *6*, 1686−1692.
(37) Li, L. L.; Tang, F. Q.; Liu, H. Y.; Hao, N. J.; Chen, D.; Teng, X.; He, J. Q. *in vivo* Delivery of Silica Nanorattle Encapsulated Docetaxel for Liver Cancer Therapy with Low Toxicity and High Efficacy. *ACS Nano* **2010**, *4*, 6874−6882.

DOI: 10.1021/am507798d
ACS Appl. Mater. Interfaces 2015, 7, 1355−1363